**Proceedings of the ASME 2021**
**International Design Engineering Technical Conferences and**
**Computers and Information in Engineering Conference**
**IDETC-CIE2021**
**August 17-19, 2021, Virtual, Online**

**DETC2021-71447**

# SIMULATION OF CORONA ELECTROSTATIC SEPARATOR FOR END-OF-LIFE MANAGEMENT IN PRINTED CIRCUIT BOARDS

**Trunal Patil[1], Lara Rebaioli[1], Irene Fassi[1]**
[1]STIIMA-CNR, Institute of Intelligent Industrial Technologies and Systems for Advanced Manufacturing,
Consiglio Nazionale delle Ricerche,
Milan, Italy

## ABSTRACT

*Printed circuit boards (PCBs) are made of several materials, including platinum, gold, silver, and rare earth elements, which are very valuable from a circular economy perspective. The PCB end of life management starts with the component removal, then the PCBs are shredded into small particles. Eventually, different separation methods are applied to the pulverized material to separate metals and non-metals. The corona electrostatic separation is one of the methods that can be used for this purpose since it is able to separate the conductive and non-conductive materials. However, the lack of knowledge to set the process parameters may affect the efficiency of the corona electrostatic separation process, ultimately resulting in the loss of valuable materials. The simulation of particle trajectory can be very helpful to identify the effective process parameters of the separation process. Thus, in this study, a simulation model to predict the particles trajectories in a belt type corona electrostatic separator is developed with the help of COMSOL Multiphysics and MATLAB software. The model simulates the particle behavior taking into account the electrostatic, gravitational, centrifugal, electric image, and air drag forces. Moreover, the predicted particles trajectories are used to analyze the effects of the roll electrode voltage, angular velocity of roll electrode, and size of the particles on the separation process.*

Keywords: End of Life management, Printed Circuit Boards, Corona Electrostatic Separation, Particle Trajectory Simulation.

## NOMENCLATURE

| | |
|---|---|
| $a_i$ | Particle acceleration at the i$^{th}$ step |
| $C_f$ | Friction coefficient |
| $E$ | Electrostatic field |
| $e_0$ | Air dielectric constant |
| $\sum F$ | Total force acting on particles |
| $F_a$ | Air drag force acting on particles |
| $F_{cc}$ | Centrifugal force acting on particles (conveyor) |
| $F_{cr}$ | Centrifugal force acting on particles (roll electrode) |
| $F_e$ | Electrostatic force |
| $F_g$ | Gravitational force acting on particles |
| $F_i$ | Electric image force acting on particles |
| $g$ | Gravitational acceleration |
| $m$ | Particle mass |
| $m_c$ | Conductive particle mass |
| $m_{nc}$ | Non-conductive particle mass |
| $n$ | Normal vector to surfaces |
| $p_i$ | Particle position at the i$^{th}$ step |
| $Q_{nc}$ | Corona charge |
| $Q_c$ | Electrostatic induction |
| $R_c$ | Conveyor radius |
| $R_r$ | Roll electrode radius |
| $r$ | Particle radius |
| $S$ | Perpendicular surface |
| $V$ | Voltage of roll electrode |
| $v$ | Particle velocity |
| $v_r$ | Particles relative velocity |
| $v_i$ | Particle velocity at the i$^{th}$ step |
| $\rho$ | Air density |
| $\omega_c$ | Angular velocity of conveyor |
| $\omega_r$ | Angular velocity of roll electrode |

## 1. INTRODUCTION

Printed circuit boards (PCBs) are rich in base metals, rare earth elements and non-metal elements, which, in a circular economy perspective, could be used as secondary materials.

Therefore, an efficient separation is very important. As shown in Figure 1, the recycling management of the PCBs starts with the removal of mounted components by using a combination of mechanical and thermal energy. After the component removal, the boards are reduced in size by a commonly used shredding procedure. The shredding of PCBs includes the machine and hammer mill. Eventually, materials are separated into the metallic and non-metallic materials by using different separation methods [1]. There are many separation methods, exploiting different physical principles, including gravity, magnetic, triboelectrostatic, and electrostatic forces. The gravity separation method is based on the specific gravity to separate the heavy and light material. The magnetic [2], electrostatic [3], and triboelectrostatic [4] separation methods are based on the magnetic field, electric conductivity, and dielectric constant, respectively.

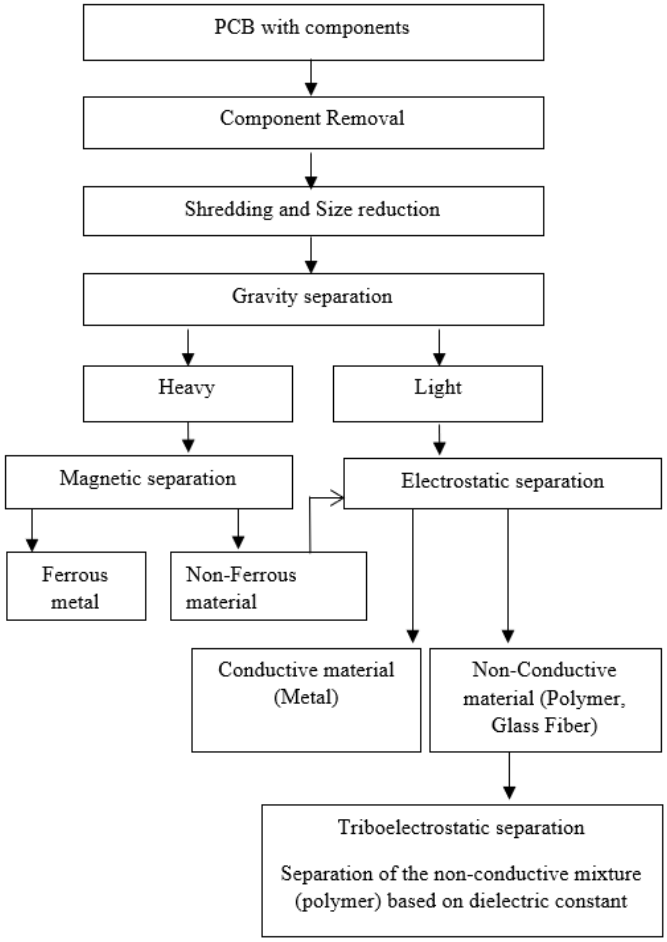


**FIGURE 1:** SEPARATION PROCESS OVERVIEW

The gravity separation is not efficient for treating smaller materials. Similarly, the magnetic separators must be regularly maintained and wiped down to detach magnetic materials that have piled up. Furthermore, the magnetic separation is only suitable to separate the magnetic and non-magnetic materials. The limitation of the triboelectrostatic separator is that it can be used only for extracting the non-conductive materials. Conversely, the electrostatic separation method is able to separate the conductive and non-conductive particles [5]. PCBs consist of a combination of the conductive and non-conductive materials and shredded PCB particles have a small size. In order to separate this combination of mixed small particles, the electrostatic separation is more suitable than the other listed separation methods. Additionally, electrostatic separation does not have a negative impact on the environment.

In the past, numerous researchers have developed several processes for electrostatic separation based on corona charge and electrostatic induction, such as the corona roll type electrostatic separation, the belt type corona electrostatic separation, the free fall electrostatic separation, and the plate type electrostatic separation processes [6,7]. The belt type corona electrostatic separation is based on the electrophoresis principle that uses the electric charge and electrostatic induction to separate conductive and non-conductive materials. When the materials pass through an electrical field, the particles acquire and lose their charge depending on their own conductivity characteristics and are separated. The conductive particles are separated by the electrostatic induction while the non-conductive particles are separated using the corona charge.

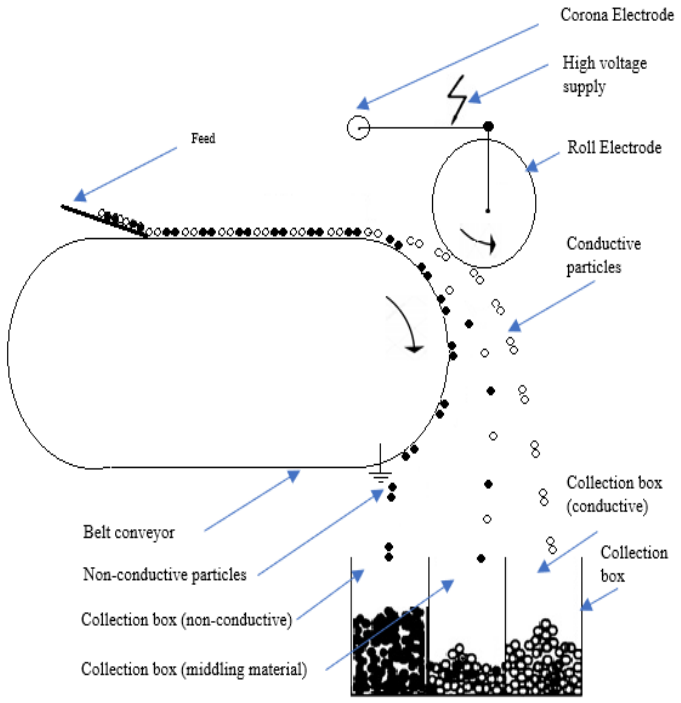


**FIGURE 2:** SCHEMATIC REPRESENTATION OF THE BELT TYPE CORONA ELECTROSTATIC SEPARATOR

Figure 2 shows the schematic representation of the belt type corona electrostatic separator. The separation is carried out by the electric field created between a roll electrode and the grounded conveyor electrode, which are both connected to a high

voltage supply. The particles to be separated are transferred on the belt conveyor by the feeder and charged by the corona electrode which is located above the conveyor. The particles behaviour changes with respect to their own characteristics, and only the non-conductive particles are able to conserve their charge. Therefore, the non-conductive particles stick to the conveyor because of the image electric force and are stored in the non-conductive or middling material collection box depending on the values of the gravitational force and image electric force. The conductive particles drop their charge through the grounded conveyor and when pass through the roll electrode area, they gain the electrostatic induction which is created by the roll electrode. Due to this fact, the conductive particles are attracted towards the roll electrode and stored in the conductive material collection box. It should be noted that the electrostatic induction does not affect the non-conductive particles. The middling box is used to store the mixture of conductive and non-conductive materials that is not separated due to non-uniform electrical field.

The belt type corona electrostatic separation is very promising, but there are still some significant problems to be solved, such as the noticeable amount of middling products. This problem is mainly due to variations in particle size and mass, electrical field, and electrode angular velocity. Moreover, the stability of the belt type corona electrostatic separation is affected by an incorrect identification of the effective process parameters according to the different composition of the particle mixture. In the past, several approaches have been used to increase the corona electrostatic separation efficiency. Lu et al. [8] performed an empirical evaluation of the effects of the different particle shapes in the separation efficiency. Jiang et al. [9] used a fractional factorial design approach to assess the relationship between the effective process parameters (high voltage, roll velocity, position of the corona electrode and electrostatic electrode from the moving particles) and the corona electrostatic separation process efficiency. However, the fractional factorial approach implied a high number of tests and resulted in a high time consumption and uneconomical approach. Furthermore, Lu et al. [10] presented a theoretical analysis to optimize the parameters of the electrostatic separators for the spherical shape metal mixtures using a computational algorithm. Similarly, Li et al. [11] focused on the angular velocity of the roll electrode to optimize the corona electrostatic separation process through a quantitative method. Moreover, automation has been implemented in the corona electrostatic separator to improve the process productivity [12]. Samuila et al. [13] proposed a new corona electrostatic separation method to separate copper and PVC (poly vinyl chloride) mixture from the waste electric and electronic equipment. The design of experiments approach was utilized to analyze the parameters of the electrostatic separation process to increase the separation efficiency. The electrode voltage and roll electrode velocity were considered as the variable factors with the mass of the copper considered as output. Unlike other approaches, the simulation of the particle trajectory approach enables the clear representation of the output from the separation process according to particle size, mass, roll electrode velocity and electrode voltage. Therefore, it could be very effective in evaluating the effective parameters to increase the corona electrostatic separation process efficiency. However, the particle trajectory simulation involves several critical problems due to the effects of several types of forces on particles with different sizes and materials [14]. Kim et al. [15] developed a method of electrostatic separation including the pretreatments such as sieving, washing, pyrolysis, and oxidation to separate the copper and glass particles from the automobile shredding residue. In this study, the electrostatic separation performance was evaluated by the particle trajectory analysis, but factors such as centrifugal force, corona charge and electric image force acting on the particles were not considered.

In this paper, a model is developed to simulate the corona electrostatic separation process. Based on this model, the behavior of different particles in the corona electrostatic separator is simulated considering the electrostatic, gravitational, centrifugal, electric image, and air drag forces. Moreover, the simulated particles trajectories are used to investigate the effect of the electrode voltage (kV), angular velocity of roll electrode (RPM), and size of the particles on the separation process.

## 2. MATERIALS AND METHODS

In this work, a simulation model of the corona electrostatic separator has been developed to predict the particle trajectory under the effect of the various effective variables (such as electrode voltage, angular velocity of roll electrode, and size of particles) and forces.

The COMSOL Multiphysics software based on the FEM (Finite Elements Method) has been used for the evaluation of the electrostatic field in the corona electrostatic separation process. The particles trajectory and graph results are calculated with the help of MATLAB software by the Euler Cromer method [16]

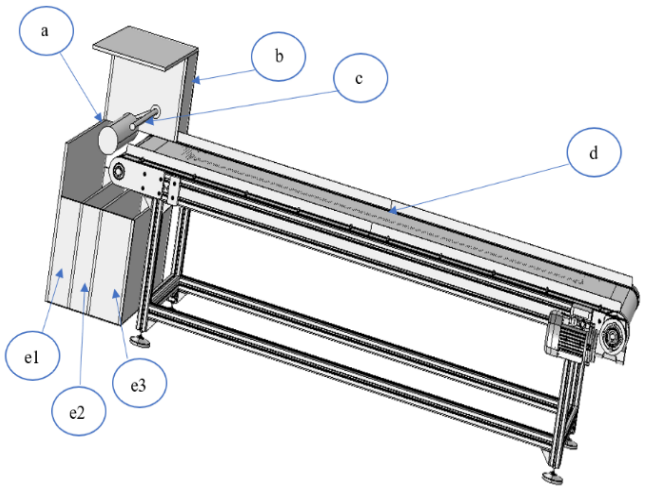


**FIGURE 3:** BELT TYPE CORONA ELECTROSTATIC SEPARATOR (a) ROLL ELECTRODE, b) HIGH VOLTAGE SUPPLY AND MOTOR, c) CORONA ELECTRODE, d) METALLIC BELT CONVEYOR, e.1) STORAGE BOX-CONDUCTING MATERIAL, e.2) STORAGE BOX-MIDDLING MATERIAL, AND e.3) STORAGE BOX- NONCONDUCTING MATERIAL)

### 2.1 Geometrical details

The geometrical model of the corona electrostatic separator used in the simulation (Figure 3) includes a metallic belt conveyor, a roll electrode, a corona electrode, high voltage supply, storage boxes for collecting the materials.

The crushed powder generated during the shredding process of printed circuit boards is transferred on a metallic belt conveyor (length and width are 1.2 m and 0.1 m, respectively) through the feeder. The roll electrode in the shape of rotating cylinder is made of stainless-steel material with radius of 30 mm. Three phase motors are used to drive the conveyor and roll electrode with VFD (variable frequency drive). The corona electrode is a tungsten wire with radius of 3 mm used to create corona discharge. A high voltage system (10 kV to 30 kV) is used to apply the voltage for the roll electrode and corona electrode.

### 2.2 Materials

In this study copper and glass fiber epoxy particles are selected since they represent the highest percentage of conductive and non-conductive material, respectively, among the waste PCB mixture [17].

The density of copper and glass fiber epoxy particles is 8940 kg/m$^3$ and 2600 kg/m$^3$, respectively. Both the copper and glass fiber epoxy particles are assumed to be spherical with a radius of 0.2 mm. The particle mass is assumed to be 0.3 mg for the copper particles and 0.1 mg for the glass fiber epoxy particles for this radius value [18].

### 2.3 Model assumptions

Several assumptions are considered to develop the model of the corona electrostatic separator. The collisions between copper and glass fiber epoxy are assumed as negligible thus this triboelectric effect is not considered. The dielectrophoretic force has negligible effects in the considered electrode configuration, thus it is neglected during the simulation trials. The adhesion force is neglected since it is more effective in the case of micrometric particles, but for the particles with a 0.2 mm size it is significantly smaller than the electric field and electric image forces. The influence of Coulomb forces between copper and glass fiber epoxy is neglected as these forces are significantly smaller than the electrical field [10, 19, 20].

### 2.4 Mathematical models

To emulate the nature of particles in the corona electrostatic separation process the following forces acting on the moving particles are considered in the model.

- The movement equation of each particle can be expressed as:

$$m\frac{dv}{dt} = \sum F \tag{1}$$

where $m$ is the mass of the particle, $v$ is its velocity, and $\sum F$ is the total force acting on particles.

- Electrostatic field acting on particles:

$$E = -\nabla V \tag{2}$$

where $E$ is electrostatic field, and $V$ represents the voltage supplied to the roll electrode.

- Corona charge: when a spherical particle passes through the conveyor and corona electrode, it is affected by the electric charge:

$$Q_{nc} = 12\pi e_0 E r^2 \tag{3}$$

where $Q_{nc}$ represents the corona charge, $e_0$ is the air dielectric constant, $E$ is the ionized electrical field, $r$ is the particle radius [19].

- Electrostatic induction: when a spherical particle passes through the conveyor and roll electrode, it is affected by the electrostatic induction

$$Q_c = \frac{2}{3}\pi^3 e_0 E r^2 \tag{4}$$

where $Q_c$ is the electrostatic induction, $e_0$ is the air dielectric constant, $E$ is the ionized electrical field, $r$ is the particle radius [10].

- Gravitational force acting on particles:

$$F_g = mg \tag{5}$$

where $F_g$ is the gravitational force, $m$ is the particle mass, and $g$ the gravitational acceleration (9.8 m/s$^2$) [21].

- Electrostatic force:

$$F_e = QE \tag{6}$$

where $F_e$ is the electrostatic force, $Q$ is the corona charge $Q_{nc}$ for non-conductive materials or the electrostatic induction $Q_c$ for conductive materials, and $E$ is the electrostatic field [21].

- Centrifugal forces acting on particles:

$$F_{cc} = m{\omega_c}^2 R_c n \tag{7}$$

where $F_{cc}$ is the centrifugal force generated by the conveyor, $m$ is the particle mass, $\omega_c$ is the angular velocity of the conveyor, $R_c$, is the radius of conveyor, and $n$ is the vector normal to the conveyor surface.

$$F_{cr} = m{\omega_r}^2 R_r n \tag{8}$$

where $F_{cr}$ is the centrifugal force generated by the roll electrode, $m$ is the particle mass, $\omega_r$ is the angular velocity of the roll electrode , $R_r$ is the radius of the roll electrode, and $n$ is the vector normal to the roll electrode surface [21].

- Electric image force acting on particles:

$$F_i = \frac{Q^2 n}{4\pi e_0 (2r)^2} \tag{9}$$

where $F_i$ is the electric image force, $Q$ is the corona charge $Q_{nc}$ for non-conductive materials or the electrostatic

induction $Q_c$ for conductive materials, $n$ is the vector normal to conveyor surface, and $e_0$ is the air dielectric constant [8].

- Air drag force acting on particles:

$$F_a = -\frac{1}{2} C_f S \rho v_r^2 \tag{10}$$

where $F_a$ is the air drag force, $C_f$ is the drag coefficient, $\rho$ is the air density, $S$ is the frontal area, and $v_r$ is the particle relative velocity [22].

### 2.5 Particle trajectory calculation

The copper and glass fiber epoxy are subjected to different forces according to their conductivity characteristics and locations. The particle movement is obtained by equation (1) including all the forces acting on the particles, namely the gravitational force (equation (5)), the electrostatic force (equation (6)), the centrifugal force (equation (7) and (8)), the electric image force (equation (9)), and the air drag force (equation (10)).

The glass fiber epoxy particles are non-conductive, hence they are not attracted by the roll electrode, but stick to the conveyor. In this case equation (1) can be expressed as:

$$\frac{dv}{dt} = a = \frac{1}{m_{nc}}\left(Q_{nc}E + m_{nc}\omega_c{}^2 R_c n + \frac{Q_{nc}{}^2 n}{4\pi e_0 2r^2} + -\frac{1}{2} C_f S \rho v_r^2 + m_{nc} g\right) \tag{11}$$

where the non-conductive particle mass ($m_{nc}$) is the mass of the glass fiber epoxy particle.

When considering the conductive copper particles that are attracted by the roll electrode, equation (1) can be expressed as:

$$a = \frac{1}{m_c}\left(Q_c E + m_c\omega_c{}^2 R_c n + m_c\omega_r{}^2 R_r n + \frac{Q_c{}^2 n}{4\pi e_0 2r^2} + -\frac{1}{2} C_f S \rho v_r^2 + m_c g\right) \tag{12}$$

where the conductive particle mass ($m_c$) is the mass of the copper particle.

After obtaining the acceleration, the positions of the copper and glass fiber epoxy particles during their movement are calculated by the Euler Cromer method:

$$v_{i+1} = v_i + a_i \delta t \tag{13}$$

$$p_{i+1} = p_i + v_{i+1} \delta t \tag{14}$$

where $v_i$ is the particle velocity at the $i^{th}$ iteration step, $a_i$ is the particle acceleration at the $i^{th}$ step, and $p_i$ is the particle position at the $i^{th}$ step.

At each iteration step the acceleration starting value is estimated by using the electrostatic field data provided by the COMSOL Multiphysics model. For this purpose, the electrostatic field values are provided to MATLAB that solves equation (11) or (12) according to the particle material. Then, based on the calculated acceleration starting value, equations (13) and (14) are used by MATLAB to identify the velocity and position at each time increment.

Figure 4 shows a block diagram that summarizes the proposed method.

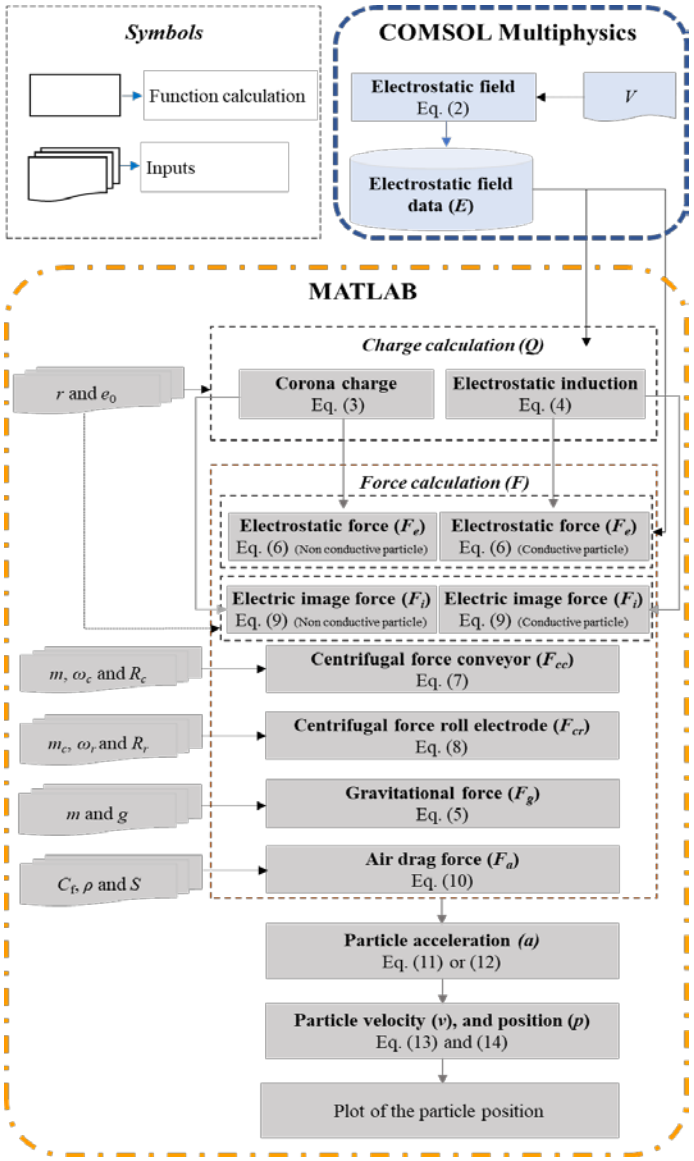


**FIGURE 4:** BLOCK DIAGRAM OF THE PROPOSED METHOD

## 3. RESULTS AND DISCUSSION

Table 1 lists the parameters that are considered as constant throughout the simulations. The initial velocity of the particle is assumed to be the same as the conveyor velocity, which is 1 m/min [23].

**TABLE 1:** CONSTANT PARAMETERS FOR THE SIMULATIONS

| | |
|---|---|
| Initial particle velocity, $v$ | 1 m/min |
| Drag coefficient, $C_f$ | 0.5 [24] |
| Air density, $\rho$ | 1225 kg/m$^3$ |
| Gravitational acceleration, $g$ | 9.8 m/s$^2$ |

Three simulation trials are carried out to identify the effect of parameters such as electrode voltage, electrode velocity, size and mass of the particles on the separation process. The input parameters are different in each simulation trial and their values are based on previous studies (Tables 2-4). Input such as electrode voltage are given to COMSOL Multiphysics. Inputs such as particle size, particle mass, and angular velocity of the electrode are given to MATLAB (Figure 4).

In these different simulation trials, the ideal distance for the separation of the copper particles is +0.05 m to +0.1 m x-distance after the conveyor, i.e. 0.15 m to 0.2 m on the reference system of Figures 5-7. Similarly, for glass fiber epoxy particles -0.05 m to 0 m x-distance after the conveyor is ideal for the separation, corresponding to 0.05 m to 0.1 m on the reference system of Figures 5-7. However, the appropriate distance depends on the size of the conductive, middling, and non-conductive collection box but also on the types and relative quantities of the mixed material, and on the size and mass of the particles.

**Simulation 1** – Particle trajectory at a different value of roll electrode angular velocity ($\omega_r$).

The input parameter constant values are listed in Table 2.

**TABLE 2:** INPUT PARAMETER CONSTANT VALUES FOR SIMULATION 1

| | |
|---|---|
| Electrode applied voltage, $V$ | 20 kV [25] |
| Copper particle size (radius), $r$ | 0.2 mm [18] |
| Glass fiber epoxy particle size (radius), $r$ | 0.2 mm [18] |
| Copper particle mass, $m$ | 0.3 mg [18] |
| Glass fiber epoxy particle mass, $m$ | 0.1 mg [18] |

The trajectories of copper and glass fiber epoxy particles at an electrode angular velocity of 12, 15 and 30 RPM are depicted in Figure 5. At 12 RPM, the glass fiber epoxy particles are attached to the conveyor while the copper particles are attracted to the electrode roll. Similarly, at 15 RPM, the glass fiber epoxy particles partially attached to the conveyor while the copper particles are a little attracted towards the roll electrode. At 30 RPM, the separation is not successful and both particles are projected towards one material collection box.

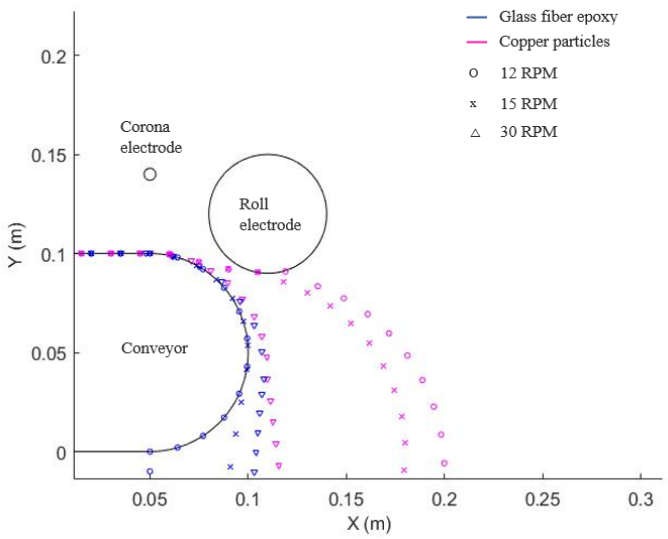


**FIGURE 5:** PARTICLE TRAJECTORY AT A DIFFERENT VALUE OF ROLL ELECTRODE ANGULAR VELOCITY ($\omega_r$ = 12 RPM, 15 RPM, AND 30 RPM)

These results point out that an increase in the electrode angular velocity results in a reduction in the conductive particle attachment to the electrode. Indeed, in this case the separation process is mainly affected by the centrifugal force. According to equation (7) and (8), increasing the value of electrode velocity, ultimately increases the centrifugal force value. At high centrifugal force values, the conductive copper particles do not stick to the roll electrode, because they are prevented from passing through the electrostatic field created by the roll electrode and do not get enough electric charge to separate from glass fiber epoxy particles.

**Simulation 2** – Particle trajectory at a different value of roll electrode voltage ($V$).

The input parameter constant values are listed in Table 3.

**TABLE 3:** INPUT PARAMETER CONSTANT VALUES FOR SIMULATION 2

| | |
|---|---|
| Electrode angular velocity, $\omega$ | 12 RPM [26] |
| Copper particle size (radius), $r$ | 0.2 mm [18] |
| Glass fiber epoxy particle size (radius), $r$ | 0.2 mm [18] |
| Copper particle mass, $m$ | 0.3 mg [18] |
| Glass fiber epoxy particle mass, $m$ | 0.1 mg [18] |

Figure 6 shows the trajectories of copper and glass fiber epoxy particles at an electrode voltage 10, 20 and 30 kV. At 10 kV, the glass fiber epoxy particles are attached to the conveyor, while the copper particles are not completely attracted towards the roll electrode. Similarly, at 20 kV, the glass fiber epoxy particles and the copper particles are attached to the conveyor and roll electrode, respectively. At 30 kV of electrode

voltage, the copper particles are strongly attracted towards the roll electrode, while the glass fiber epoxy particles are not attracted towards the conveyor. Separation is best performed at 20 kV because both particles have maintained their trajectories with a suitable distance both and are projected to the corresponding collection box.

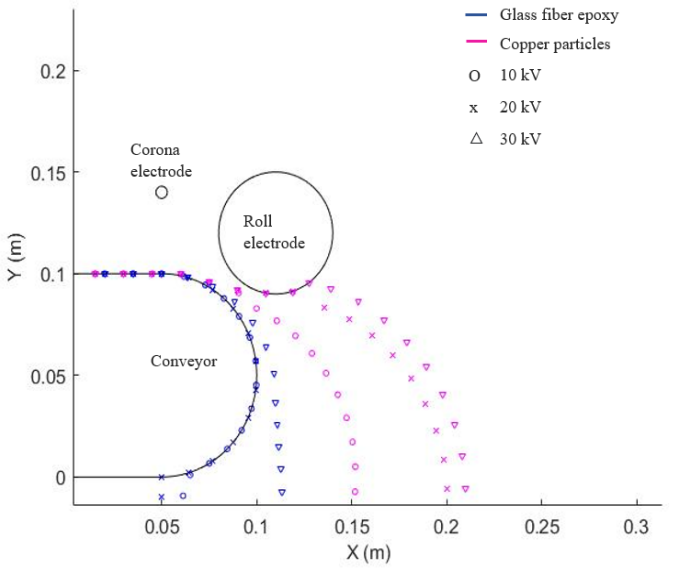


**FIGURE 6:** PARTICLE TRAJECTORY AT A DIFFERENT VALUE OF ROLL ELECTRODE VOLTAGE ($V$ = 10 kV, 20kV AND 30 kV)

In this case, the results prove that the force having the greatest influence on the separation process is the electrostatic force. An increase in the roll electrode voltage results in a higher sticking of the conductive particles to the electrode, thus the voltage should be carefully adjusted to project the particles exactly to the suitable collection box.

**Simulation 3** – Particle trajectory at a different value of particle size ($r$).

The input parameter constant values are listed in Table 4. In this case, the particle mass changes according to the radius.

**TABLE 4:** INPUT PARAMETER CONSTANT VALUES FOR SIMULATION 3

| | |
|---|---|
| Electrode applied voltage, $V$ | 20 kV [25] |
| Electrode angular velocity, $\omega$ | 12 RPM [26] |

The trajectories of copper and glass fiber epoxy particles at a particle radius of 0.1, 0.2 and 0.4 mm are depicted in Figure 7. At 0.1 mm, the sticking of both conductive and non-conductive particles is strong. At 0.2 mm, the glass fiber epoxy particles are attached to the conveyor and the copper particles are projected towards the conductive material box, thus the particle separation is successful. At 0.4 mm, the glass fiber epoxy particles are partially attached to the conveyor and the copper particles are not attracted towards the roll electrode.

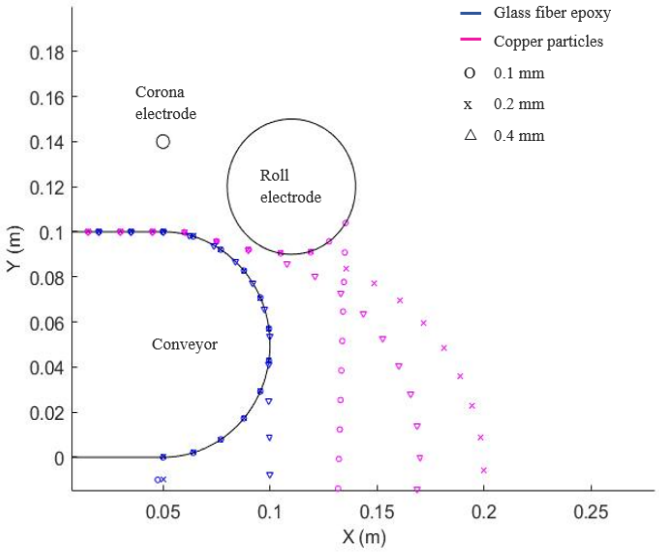


**FIGURE 7:** PARTICLE TRAJECTORY AT A DIFFERENT VALUE OF PARTICLE RADIUS ($r$ = 0.1 mm, 0.2 mm AND 0.4 mm)

Under the effect of electric image force, the charged particles are attached to the conveyor and roll electrode according to the Coulomb attraction between a charge of the particle acquired and its image (-$Q$) located at a distance 2$r$ from it. Thus, a higher particle radius causes a decrease in the electric image force and in the particle attachment. Also, an increase in the radius of the particles results in an increase of their mass and, thus, the centrifugal force generated by the conveyor and roll electrode, and gravitational forces increase according to $r^3$. Therefore, if the particle radius becomes higher, the centrifugal and gravitational forces prevail over the electrostatic force. In conclusion, when the particle radius increases, the sticking of non-conductive particles to the conveyor decreases, while in the case of the conductive particles, the sticking to the roll electrode decreases, and the electrostatic force becomes weaker compared to the other contributing forces.

## 4. CONCLUSIONS

In this paper a preliminary simulation model of the corona electrostatic separator has been developed. Based on this model, the effective parameter like electrode voltage (kV), angular velocity of roll electrode (RPM), and size of the particles in the corona electrostatic separator have been analyzed. The results have highlighted that the identification of effective parameters according to different particles in the mixture is very important in order to improve the efficiency of the corona electrostatic separation process.

The preliminary model is simplified and includes only two particles of different materials, namely, copper and fiber glass epoxy, whose shape is assumed to be spherical. Moreover, the

adhesion force between particles is neglected. In order to improve the simulation performance, future works will aim at considering several particle materials such as base metals (iron, aluminum, nickel, and zinc), rare earth elements (gold, silver and platinum), and non-metals (polymer and different glass fiber) that can be found in waste printed circuit boards. Similarly, different particle structures like spherical, cylindrical, and flake shapes will be incorporated in the current simulation model. In addition to that, further studies will focus on including the interaction between the particles and the adhesion force.

Further studies will also aim at performing suitable experimental campaigns to validate the model by comparing the simulation results and experimental results.

Moreover, based on the simulation model, a suitable virtual management system could be developed to control and monitor the corona electrostatic separation by an online identification of the effective parameters with the help of a real time material characterization technique (hyperspectral image analysis) providing the information about the materials that are present in the waste PCBs.

## ACKNOWLEDGEMENTS

This work has been developed in the context of the H2020-MSCA-ITN DiManD project funded by the European Union's Horizon 2020 research and innovation program under the grant agreement no. 814078.

## REFERENCES

[1] X. Zeng, L. Zheng, H. Xie, B. Lu, K. Xia, K. Chao, W. Li, J. Yang, S. Lin, J. Li, Current Status and Future Perspective of Waste Printed Circuit Boards Recycling, Procedia Environ. Sci. 16 (2012) 590–597 https://doi.org/10.1016/j.proenv.2012.10.081.

[2] J. Oberteuffer, Magnetic separation: A review of principles, devices, and applications, IEEE Trans. Magn. 10 (1974) 223–238. https://doi.org/10.1109/TMAG.1974.1058315.

[3] C.B. Gill, Electrostatic Separation BT- Materials Beneficiation, in: C.B. Gill (Ed.), Springer New York, New York, NY, 1991: pp. 141–147. https://doi.org/10.1007/978-1-4612-3020-5_8.

[4] M. Mirkowska, M. Kratzer, C. Teichert, H. Flachberger, Principal Factors of Contact Charging of Minerals for a Successful Triboelectrostatic Separation Process – a Review, BHM Berg- Und Hüttenmännische Monatshefte. 161 (2016) 359–382. https://doi.org/10.1007/s00501-016-0515-1.

[5] C.-H. Park, H.-S. Jeon, H.-S. Yu, O.-H. Han, J.-K. Park, Application of Electrostatic Separation to the Recycling of Plastic Wastes: Separation of PVC, PET, and ABS, Environ. Sci. Technol. 42 (2008) 249–255. https://doi.org/10.1021/es070698h.

[6] L. Dascalescu, T. Zeghloul, A. Iuga, Chapter 4 - Electrostatic Separation of Metals and Plastics From Waste Electrical and Electronic Equipment, in: A. Chagnes, G. Cote, C. Ekberg, M. Nilsson, T.B.T.-W.R. Retegan (Eds.), Elsevier, 2016: pp. 75–106. https://doi.org/10.1016/B978-0-12-803363-0.00004-3.

[7] Y. Higashiyama, K. Asano, Recent progress in electrostatic separation technology, Part. Sci. Technol. 16 (1998) 77–90. https://doi.org/10.1080/02726359808906786.

[8] H. Lu, J. Li, J. Guo, Z. Xu, Movement behavior in electrostatic separation: Recycling of metal materials from waste printed circuit board, J. Mater. Process. Technol. 197 (2019) 101–108. https://doi.org/10.1016/j.jmatprotec.2007.06.004.

[9] W. Jiang, L. Jia, X. Zhen-ming, Optimization of key factors of the electrostatic separation for crushed PCB wastes using roll-type separator, J. Hazard. Mater. 154 (2019) 161–167. https://doi.org/10.1016/j.jhazmat.2007.10.018.

[10] H.-Z. Lu, J. Li, J. Guo, Z.-M. Xu, Dynamics of spherical metallic particles in cylinder electrostatic separators /purifiers., J. Hazard. Mater. 156 (2019) 74–79. https://doi.org/10.1016/j.jhazmat.2007.11.109.

[11] J. Li, H. Lu, Z. Xu, Y. Zhou, Critical rotational speed model of the rotating roll electrode in corona electrostatic separation for recycling waste printed circuit boards., J. Hazard. Mater. 154 (2018) 331–336. https://doi.org/10.1016/j.jhazmat.2007.10.030.

[12] J. Li, Q. Zhou, Z. Xu, Real-time monitoring system for improving corona electrostatic separation in the process of recovering waste printed circuit boards., Waste Manag. Res. 32 (2018) 1227–1234. https://doi.org/10.1177/0734242X14554647.

[13] A. Samuila, L. Dascalescu, L. Calin, M. Bilici, A. Catinean, Recent researches in electrostatic separation technologies for the recycling of waste electric and electronic equipment, AIP Conf. Proc. 2218 (2020) 30001. https://doi.org/10.1063/5.0001074.

[14] M. Remadnia, M. Kachi, S. Messal, A. Oprean, X. Rouau, L. Dascalescu, Electrostatic Separation of Peeling and Gluten from Finely Ground Wheat Grains, Part. Sci. Technol. 32 (2014) 608–615. https://doi.org/10.1080/02726351.2014.943379.

[15] B.-U. Kim, C.-H. Park, Electrostatic Separation of Copper and Glass Particles in Pretreated Automobile Shredder Residue, Metals (Basel). 8 (2018). https://doi.org/10.3390/met8110879.

[16] H. Gould, J. Tobochnik, W. Christian, E. Ayars, An Introduction to Computer Simulation Methods: Applications to Physical Systems, 2nd Edition, Am. J. Phys. - AMER J PHYS. 74 (2006) 652–653. https://doi.org/10.1119/1.2219401.

[17] I. de Marco, B.M. Caballero, M.J. Chomón, M.F. Laresgoiti, A. Torres, G. Fernández, S. Arnaiz, Pyrolysis of electrical and electronic wastes, J. Anal. Appl. Pyrolysis. 82 (2008) 179–183. https://doi.org/10.1016/j.jaap.2008.03.011.

[18] P. Oliveira, F. Taborda, C. Nogueira, F. Margarido, The Effect of Shredding and Particle Size in Physical and Chemical Processing of Printed Circuit Boards Waste, Mater. Sci. Forum. 730–732 (2012) 653–658. https://doi.org/10.4028/www.scientific.net/MSF.730-732.653.

 

[19] G. Richard, A. Ragab, K. Medles, C. Lubat, S. Touhami, L. Dascalescu, Experimental and Numerical Study of the Electrostatic Separation of Two Types of Copper Wires From Electric Cable Wastes, IEEE Trans. Ind. Appl. PP (2017) 1. https://doi.org/10.1109/TIA.2017.2677883.
[20] H. Lu, J. Li, J. Guo, Z. Xu, Movement behavior in electrostatic separation: Recycling of metal materials from waste printed circuit board, J. Mater. Process. Technol. 197 (2008) 101–108. https://doi.org/10.1016/j.jmatprotec.2007.06.004.
[21] M. Younes, A. Tilmatine, K. Medles, M. Rahli, L. Dascalescu, Numerical Modeling of Conductive Particle Trajectories in Roll-Type Corona-Electrostatic Separators, IEEE Trans. Ind. Appl. 43 (2007) 1130–1136. https://doi.org/10.1109/TIA.2007.904363.
[22] S. Maxemow, That's a Drag: The Effects of Drag Forces, Undergrad. J. Math. Model. One + Two. 2 (2013). https://doi.org/10.5038/2326-3652.2.1.4.
[23] Rajaonarivony, Rova Karine, Rouau, Xavier, Dascalescu, Lucien, Mayer-Laigle, Claire, Electrostatic separation of mineral and vegetal powders with a custom built corona separator: application to biorefinery of rice husk, EPJ Web Conf. 140 (2017) 13020. https://doi.org/10.1051/epjconf/201714013020.
[24] T. engineering Toolbox, The Engineering Toolbox, (2010) 1. https://www.engineeringtoolbox.com/drag-coefficient-d_627.html (accessed February 8, 2021).
[25] J. Li, H. Lu, S. Liu, Z. Xu, Optimizing the operating parameters of corona electrostatic separation for recycling waste scraped printed circuit boards by computer simulation of electric field, J. Hazard. Mater. 153 (2018) 269–275. https://doi.org/10.1016/j.jhazmat.2007.08.047.
[26] B. Kim, O. Han, H. Jeon, S. Baek, C. Park, Trajectory Analysis of Copper and Glass Particles in Electrostatic Separation for the Recycling of ASR, Metals (Basel). 7 (2017). https://doi.org/10.3390/met7100434.